Materials Chemistry and Physics 143 (2013) 322–329

Contents lists available at ScienceDirect

Materials Chemistry and Physics

journal homepage: www.elsevier.com/locate/matchemphys

# In-situ hydrothermal crystallization $Mg(OH)_2$ films on magnesium alloy AZ91 and their corrosion resistance properties

Jing Feng [a, *], Yan Chen [a], Xiaohan Liu [b], Tiandi Liu [a], Linyi Zou [a], Yuting Wang [a], Yueming Ren [a], Zhuangjun Fan [a], Yanzhuo Lv [a], Milin Zhang [a]

[a] Key Laboratory of Superlight Materials & Surface Technology of Ministry of Education, Harbin Engineering University, Harbin 150001, PR China
[b] Avic Shenyang Aircraft Corporation, Shenyang 110850, PR China

## HIGHLIGHTS

- $Mg(OH)_2$ film on AZ91 was prepared by an in-situ hydrothermal method.
- $Mg(OH)_2$ films are composed of circular nano-flakes.
- The growth process of $Mg(OH)_2$ film was analyzed and illustrated.
- The $Mg(OH)_2$ film showed strong adhesion and good corrosion resistance.

## GRAPHICAL ABSTRACT

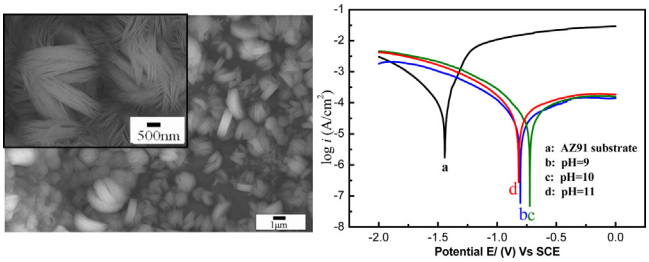


## ARTICLE INFO

*Article history:*
Received 7 September 2012
Received in revised form
13 May 2013
Accepted 3 September 2013

*Keywords:*
Alloys
Thin films
Coatings
Adhesion
Corrosion

## ABSTRACT

$Mg(OH)_2$ films have been fabricated on magnesium alloy AZ91 substrates by an in-situ hydrothermal method. AZ91 alloy substrates act as both the source of $Mg^{2+}$ ion and the support for the $Mg(OH)_2$ film in synthetic process. The effect of pH value and hydrothermal treatment time on the morphologies and corrosion resisting properties of $Mg(OH)_2$ film is studied. The obtained $Mg(OH)_2$ films are uniform and compact. The adhesion between the films and the substrate is strong due to the in-situ growth process, which enhances their potential for practical applications. Potentiodynamic polarization measurements showed that the $Mg(OH)_2$ films obtained at pH 10, 3 h exhibits the highest increase in corrosion potential at −0.7097 V and lowest $i_{corr}$, which suggests that it is the best effective film in improving the corrosion resistance of AZ91in all obtained films.



## 1. Introduction

Magnesium and its alloy have attracted great attention due to their low price, high strength-to-weight ratio and good recycling properties. They have been used widely in many fields such as in automotive, aerospace and electronics [1–3]. Furthermore, they have been considered as one of the potential implant biomaterials because of their close mechanical properties to natural bone and perfect biocompatibility [4–6]. But the poor corrosion resistance limits their applications as biomaterials gravely. Surface modification is considered as an effective technique to improve corrosion resistance of Mg alloys because surface modification can provide a barrier between the metals and their environment. It includes chromate conversion films [7], electrodeposition of hydroxyapatite films [8], cathodic electrophoretic deposition [9] and micro-arc oxidation treatment et al. [10]. Among them, chromate conversion film shows excellent corrosion resistance, but chromate is harmful due to the biological toxicity [11], which restricts the applications of chromate films as biomaterials. Micro-arc oxidation treatment films were found to contain magnesium oxide with some

* Corresponding author. Tel.: +86 451 82569890; fax: +86 451 82533026.
*E-mail address:* fengjing@hrbeu.edu.cn (J. Feng).

0254-0584/$ – see front matter © 2013 Elsevier B.V. All rights reserved.
http://dx.doi.org/10.1016/j.matchemphys.2013.09.005

of other electrolyte-borne elements ($MgF_2$, $Mg_3(PO_4)_2$ or $MgAl_2O_4$, etc.) [12–14]. However, these complex films are not beneficial to the biomaterials application for poor biocompatibility. Therefore, MgO and $Mg(OH)_2$ are applied as protecting films owing to their nontoxic and biocompatible properties. Ting Lei et al. fabricated MgO films on magnesium alloys by anodic electrodeposition [12]. F. Stippich et al. synthesized protective magnesium oxide layers by ion beam-assisted deposition [15]. Yanying Zhua et al. coated $Mg(OH)_2$ film on AZ31 by a hydrothermal method [16].

Beside the request of good biocompatibility, the film must be uniform, well adhesion strength to provide adequate corrosion protection. In-situ hydrothermal growth process can improve strong adhesion between the film and the substrate due to the presence of chemical bonding between the film and substrate [17–19]. For instance, Liu et al. fabricated layered double hydroxides (LDH) films on divalent metal substrates by a solution reaction method [17]. P. Gao et al. synthesized ZnO nanorod arrays on zinc foil by a hydrothermal method [18], Guo et al. fabricated LDH/$Al_2O_3$ bilayer film on aluminum by a one-step hydrothermal method [19]. Here, we fabricate nontoxic $Mg(OH)_2$ films directly on AZ91 substrate by a simple in-situ hydrothermal route and the resulting films inhibit corrosion of the underlying metal. In the process, the source of $Mg^{2+}$ of $Mg(OH)_2$ comes form AZ91 substrate directly owing to a in-situ growth process and resulting in the strong adhesion to the substrate.

## 2. Material and methods

### 2.1. Preparation of AZ91 substrate

Magnesium alloy (AZ91, 9% Al, 1% Zn, and Mg balance) sheets were cut into oblong strips with 20 mm × 15 mm. The substrates were ground and polished with 600, 1000, 1500 and 2000 grit silicon carbide paper to achieve a smooth surface and get rid of impurities layer on the surface until the surface was shinning, degreased with the ethanol and acetone (volume ratio 1:1) in an ultrasonic bath for 10 min, and then dried in the air.

### 2.2. Growth of $Mg(OH)_2$ film

The $Mg(OH)_2$ film was prepared by in-situ crystallization on AZ91 substrate using a hydrothermal method. Sodium dioctyl sulfosuccinate ($C_{20}H_{37}NaO_7S$ (OT), 0.6 g, Sinopharm Chemical Reagent Co., Ltd., AR) was added to deionized water (35 mL) with vigorous stirring for 30–50 min. The pH (9–11) was adjusted by NaOH (0.1 mol $L^{-1}$, Tianjin Kemiou Chemical Reagent Co., Ltd., AR). Then the solution and an AZ91 substrate were transferred into a 40 mL teflon-lined stainless. The autoclave was kept at 120 °C for 3 h–8 h, pH value from 9 to 11, in an electric oven, respectively. Finally the AZ91 substrate was washed with distilled water and absolute ethanol for several times.

### 2.3. Characterization of films

X-ray powder diffraction analysis was conducted on a TTR-III diffractometer (Rigaku, Japanese) using Cu Kα radiation ($\lambda = 0.15405$ nm) in the $2\theta$ range 10°–70°, and the step interval is 0.01°. The morphologies of the films were characterized by SEM (HITACHI S-4800). The elemental analysis of the samples was carried out using EDX equipped onto SEM. X-ray photoelectron spectroscopy (XPS) measurements were performed using a PHI 5700 ESCA spectrometer with a monochromated Al K radiation ($h\nu = 1486.6$ eV). All XPS spectra were corrected using the C 1s line at 285.1 eV. The FTIR spectrum of the surface deposits was recorded on a PerkinElmer Spectrum 100 FTIR spectrophotometer with a spectral resolution of 4 $cm^{-1}$ and accumulation of 16 scans. A three-electrode configuration was employed with the sample under test as the working electrode (1 $cm^2$), a platinum electrode as the counter electrode, and a saturated calomel electrode (SCE) as the reference electrode. NaCl aqueous solution (3.5%) was used as the electrolyte. The polarization curves were recorded with CHI 660B (Shanghai, China) at room temperature with a sweep rate of 10 mV $s^{-1}$. The samples were immersed in the corrosive medium for 30 min prior to the electrochemical tests. The adhesion of the $Mg(OH)_2$ film synthesized at pH 10 on the surface of Mg alloy was performed according to the method reported in the literature [19]. This kind of tape test was previously used to establish the adhesion of the hydrothermal film to the substrate [20].

## 3. Results and discussion

### 3.1. Effect of pH and hydrothermal time on structure and morphology

The XRD patterns of the bare AZ91 substrate and AZ91 coated with the $Mg(OH)_2$ film are shown in Fig. 1.The figures reveal the characteristic peaks of the $Mg(OH)_2$ according to Powder Diffraction Standards (JCPDS) file No. (75-1527). It is found that there are $MgAl_{26}O_{40}$ in the films which may be the product of the hydrothermal process. Peaks intensity of $Mg(OH)_2$ strengthen with the increase of treatment time. Supplement figure (SFig. 1) displays the contrasting pictures of $Mg(OH)_2$ films and the bare AZ91, there are obvious white particles and black films covering on the surfaces of AZ91. The mass of white particles increases with pH increasing.

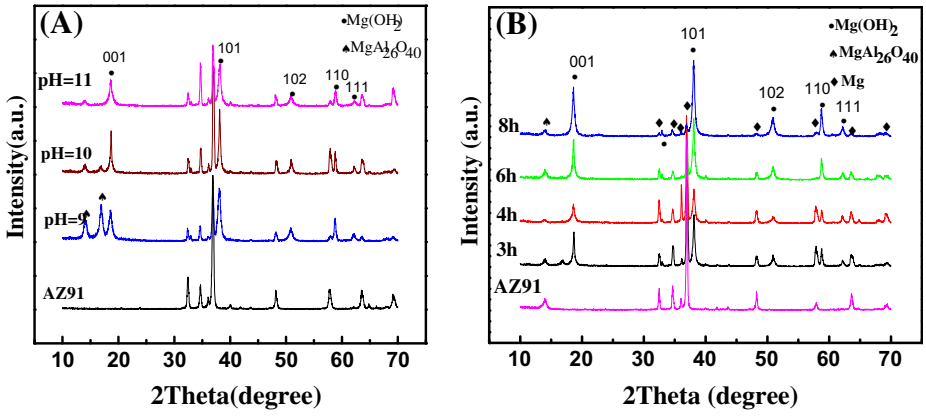


**Fig. 1.** The XRD patterns of the bare AZ91 substrate and AZ91 coated with the $Mg(OH)_2$ films, (A) with different pH values, (B) with different treating time.

SEM micrographs of the $Mg(OH)_2$ films prepared at different pH values are shown in Fig. 2. All obtained $Mg(OH)_2$ films are smooth and compact over the AZ91 substrate, and the morphologies of $Mg(OH)_2$ are strongly pH-dependent. The $Mg(OH)_2$ film obtained at pH9 covers with biscuits, which are composed of thin circular nano-flakes. These biscuits are vertical interleaved with an average diameter of 2 μm and the thickness of 900 nm. The resulting film obtained at pH10 becomes more compact and uniform. The biscuits interlace and grow together forming a compact intertexture structure like ball of strings, which provide better protection for AZ91. On the film obtained at pH11, the intertexture structure changes to incompact nano-flakes. The thickness of $Mg(OH)_2$ film tested by SEM (shown in Fig. 3) is 18 μm, 60 μm and 86 μm at pH 9, pH 10 and pH 11, respectively. The film thickness increases with the pH values. It is ascribed to the amount of $Mg(OH)_2$ accretion with the $OH^-$ concentration increasing.

The adhesion strength of anticorrosion film to the substrate is a very important factor to evaluate the film quality and determine whether the film is useful in practice. The adhesion results of the film obtained at pH 10 is shown in Fig. 3(D). There is no delamination or peeling occurred on the cross cutting surface, which indicates strong adhesion of the film to the metal substrate. This proves that the film growth directly from a substrate generally have a stronger adhesion [19]. The EDS spectra of the three different positions (1–3) in the film prepared at pH 10 h and 3 h are shown in Fig. 4. The atomic ratio between Mg and O is approximately 1:1 to 1:2, which give the evidence of the $Mg(OH)_2$ film growing successfully on the Mg alloy.

The morphologies of the films with different hydrothermal time are showed in Fig. 5. It can be observed that the amount of the magnesium alloy $Mg(OH)_2$ on the surface increasing with the increase treatment time. The film prepared with 3 h and 4 h are intense and close-grained film covered by interlaced biscuits constituted circular nano-flakes. The film synthesized with 6 h appears many cracks and the film with 8 h is very incompact, which both induce poor corrosion resistance of magnesium alloy.

### 3.2. Chemical compositions of the films

Fig. 6 shows XPS spectrum of the alloy covered with $Mg(OH)_2$ film synthesized by hydrothermal method at pH10, 3 h. The signals of C, O, Mg, S and Zn are observed from the survey XPS spectrum in Fig. 6(a). The maximum of C 1s photopeak located at 285.1 eV and was taken as a reference. Mg in metal, oxide and hydroxide environments is unambiguously identified from chemical shift observed for Mg 1s and Mg 2p peaks (and for the O 1s peak). Binding energy values of Mg 1s (1305.4 eV) and O 1s(532.4 eV) shows that Mg is mainly present as hydroxide [16,21]. The Mg K L L parameter 990.1 eV and 1003.4 eV (Fig. 4) attributed to $Mg(OH)_2$ and MgO. It can be seen that the surface compositions of $Mg(OH)_2$ film are mainly $Mg(OH)_2$ and a small amount of Si, S and Zn.

In the FTIR measurement, the $Mg(OH)_2$ deposits (obtained at pH10, 3 h)were scratched from the AZ91 substrates carefully, mixed with potassium bromide (KBr), and then compressed into

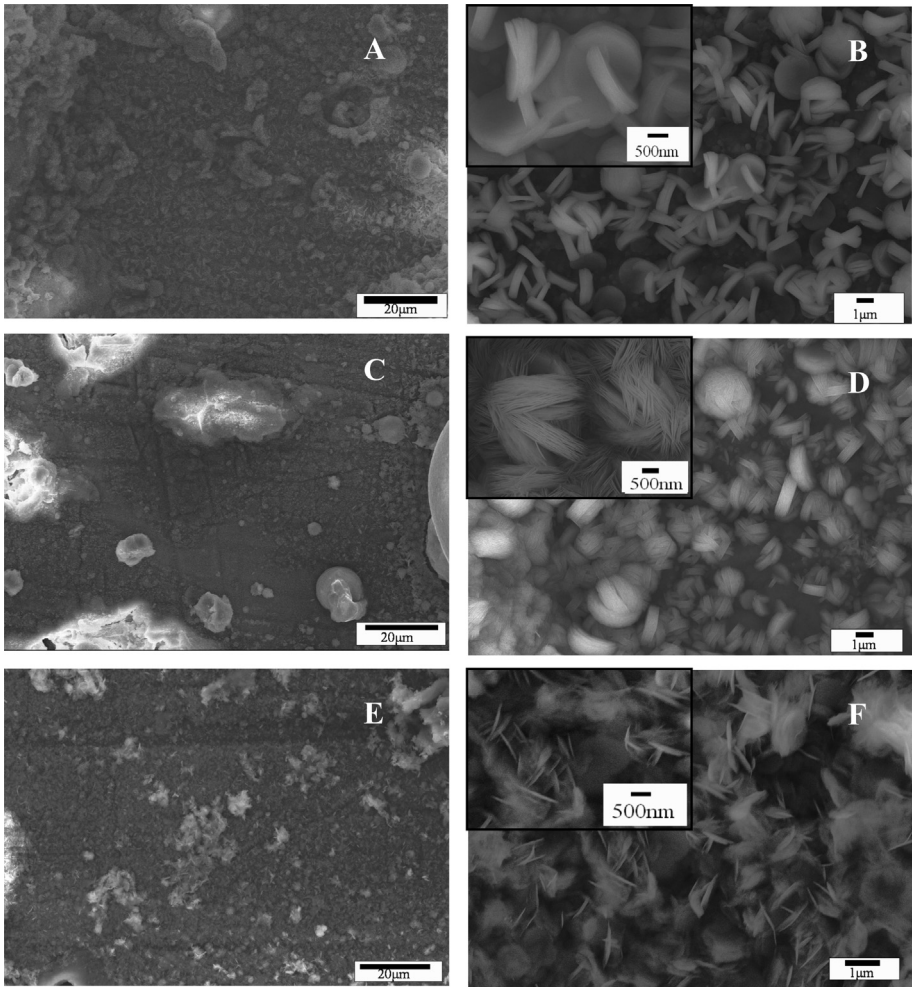


**Fig. 2.** The SEM micrographs of the $Mg(OH)_2$ films prepared on different pH value. (A–B: pH = 9; C–D: pH = 10; E–F: pH = 11).

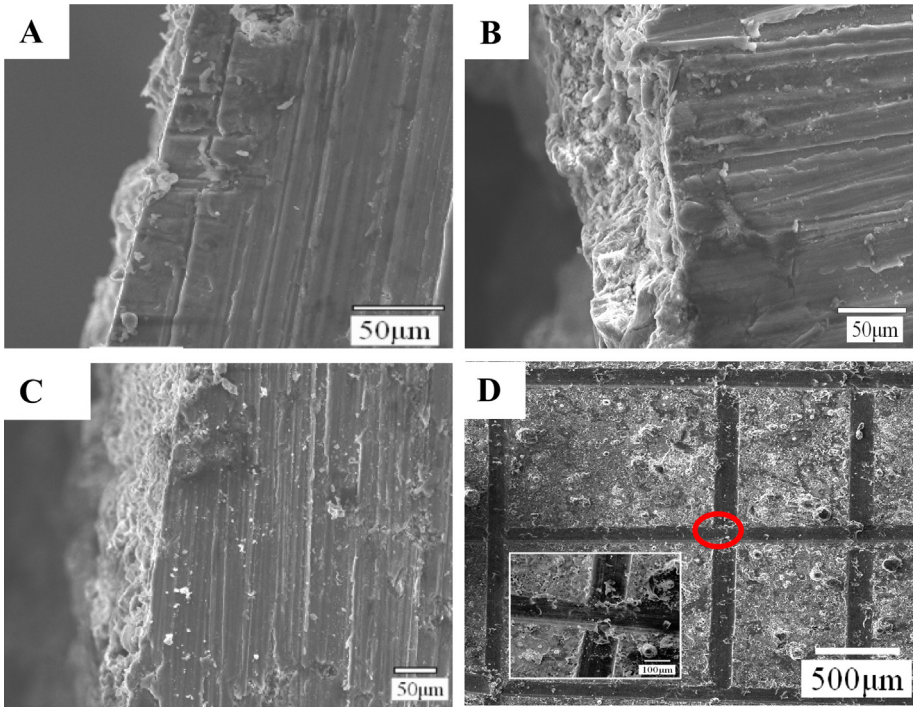


**Fig. 3.** The flanks of $Mg(OH)_2$ films obtained at different pH value (A: pH = 9; B: pH = 10; C: pH = 11). D: SEM image of $Mg(OH)_2$ film prepared at pH10 tested for adhesion.

transparent round disk. The FTIR spectrum of Mg(OH)2 film and pure $Mg(OH)_2$ is shown in Fig. 7. The spectra of $Mg(OH)_2$ film and pure $Mg(OH)_2$ powder are almost coincident, which testify that the film obtained by hydrothermal method is $Mg(OH)_2$. The peak at 3700 $cm^{-1}$ is quite sharp and strong, which can be attributed to the O–H stretching in the crystal structure of $Mg(OH)_2$. The overlaid absorption peaks in the range of 1440–1650 $cm^{-1}$ are attributed to the O–H stretching mode in water [16]. The strong band at around 445 $cm^{-1}$ is assigned to the Mg–O stretching vibration in $Mg(OH)_2$ [22].

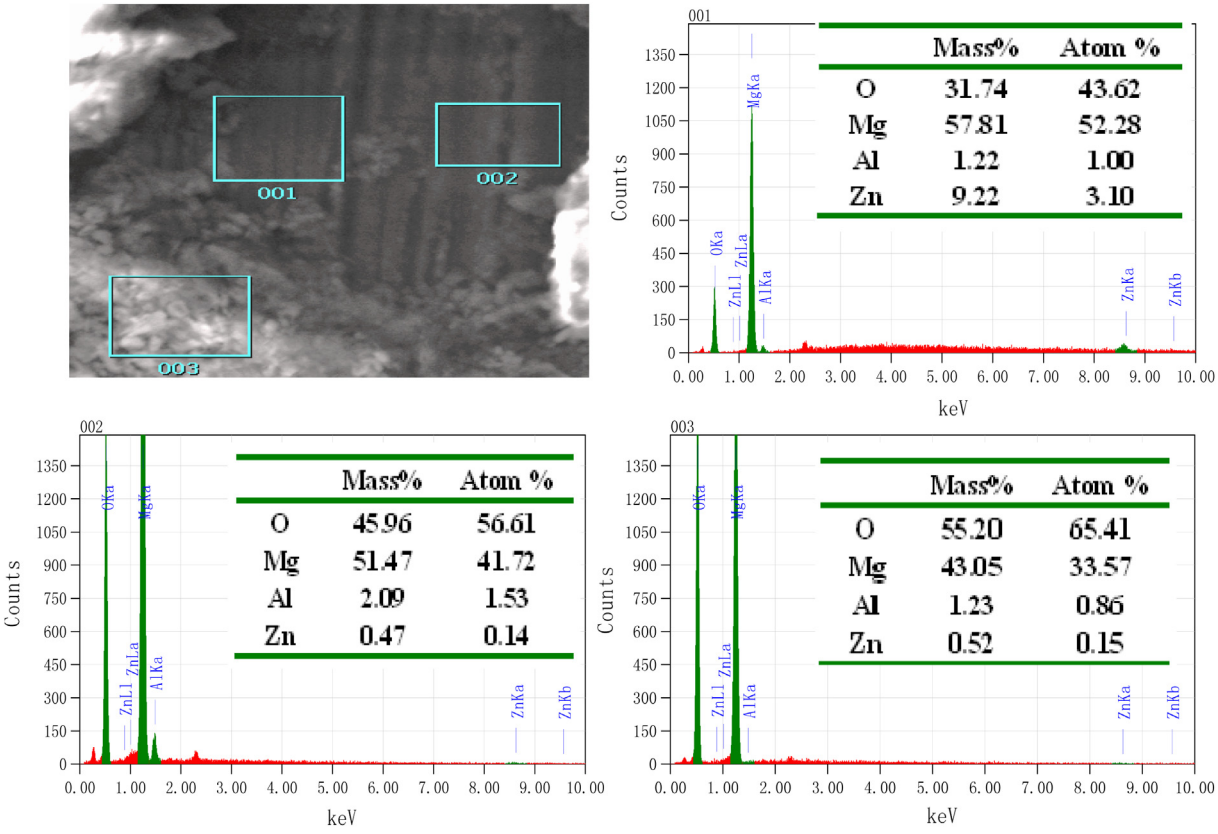


**Fig. 4.** EDS spectra of three different positions (001–003) in the $Mg(OH)_2$ film prepared at pH 10, 3 h.

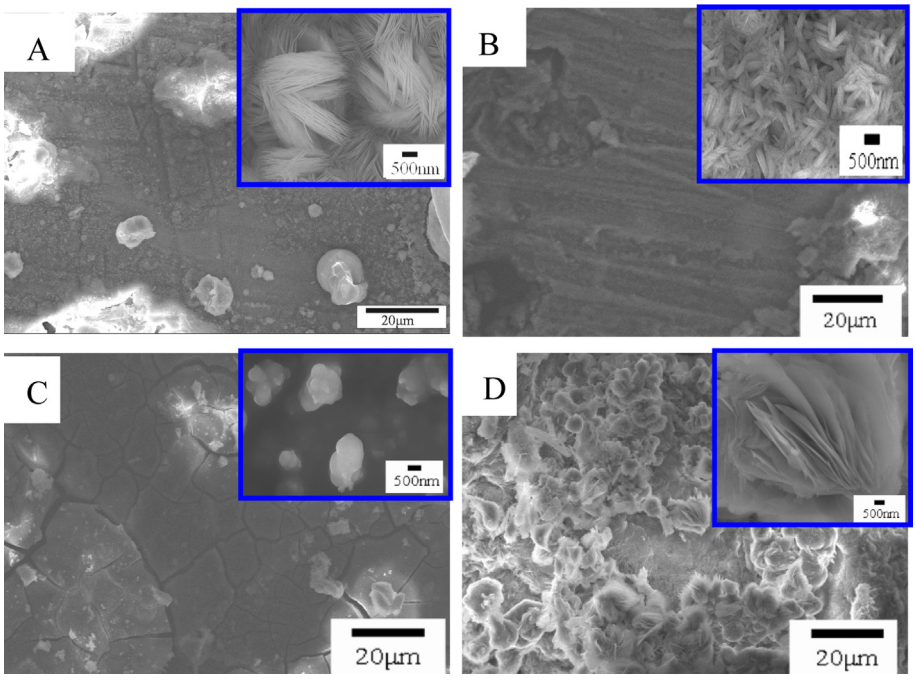


**Fig. 5.** The SEM pictures of the $Mg(OH)_2$ films prepared under different hydrothermal treating time at pH 10 (A: 3 h; B: 4 h; C: 6 h; D: 8 h).

### 3.3. Growth process of $Mg(OH)_2$ films

The growth process of $Mg(OH)_2$ films can be describe as the following formula:

$$Mg_{(surface)} \xrightarrow{OT} Mg^{2+} \quad (1)$$

$$Mg^{2+} + 2OH^- \rightarrow Mg(OH)_2 \quad (2)$$

We illustrate the process in Fig. 8. Sodium dioctyl sulfosuccinate (OT) is an anionic surfactant and generate anion headgroups when it hydrolyzing. These anion headgroups can passively adsorb onto the surface of Mg-alloy and incorporate $Mg^{2+}$ ions into their bilayer assemblies as counterions. This improves Mg atoms convert into

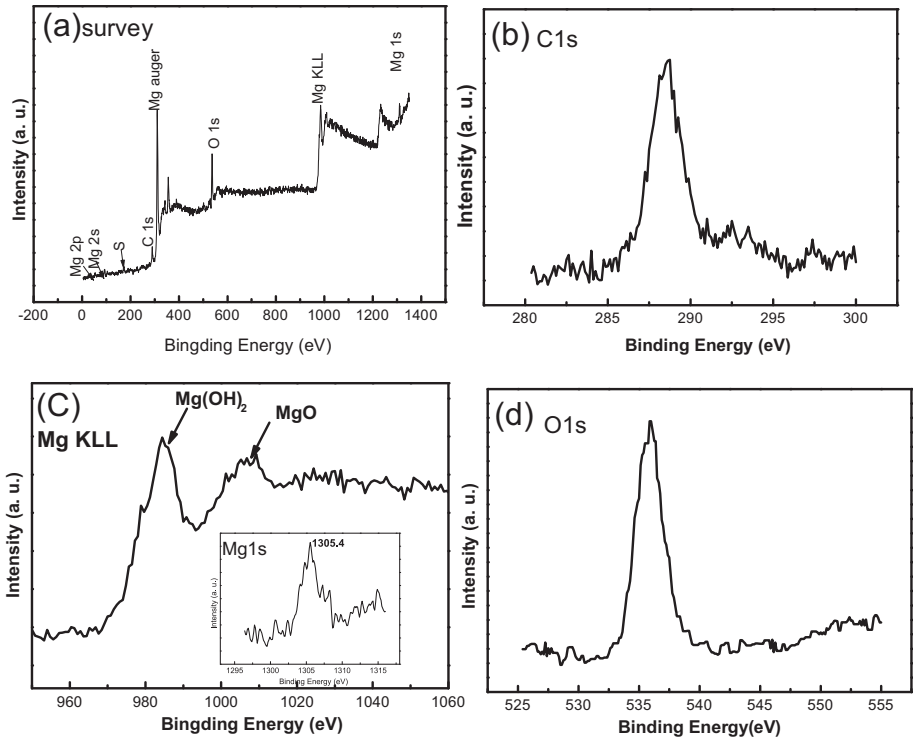


**Fig. 6.** XPS spectrum of AZ91 covered with $Mg(OH)_2$ film synthesized by hydrothermal method at pH10, 3 h. (a) survey; (b) C 1s spectrum; (c) Mg KLL spectrum and the insert is Mg 1s spectrum; (d) O 1s spectrum.

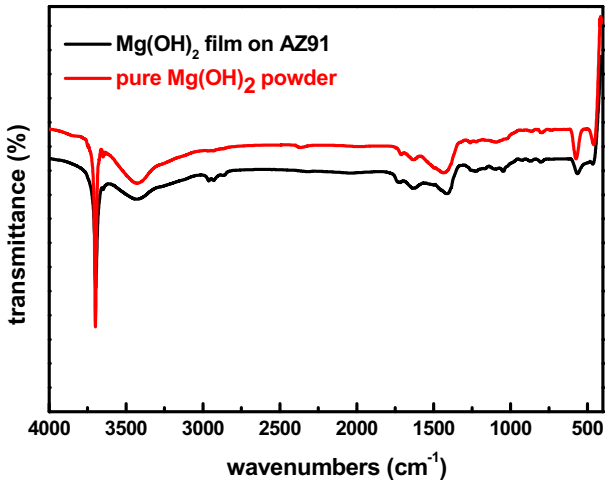


**Fig. 7.** FTIR spectra of the $Mg(OH)_2$ on AZ91 surface obtained at pH10, 3 h and pure $Mg(OH)_2$ powder.

$Mg^{2+}$, just like anionic surfactant contribute to ZnO film growth [18,23,24], as shown in Fig. 8. A part of these $Mg^{2+}$ ions diffuse into the solution and react with $OH^-$ to generate $Mg(OH)_2$ particles. These white particles of $Mg(OH)_2$ deposit on the surface of AZ91. They are poor adhesion to the substrate. The other $Mg^{2+}$ ions remain their primary stations and react with $OH^-$ in the solution, and they in-situ growth $Mg(OH)_2$ films in the surface resulting in strong adhesion to AZ91 substrate.

### 3.4. Results of immersion test

Corrosion process of magnesium and its alloy in water can be described as the following reaction:

$$Mg \rightarrow Mg^{2+} + 2e^- \text{(Anodic reaction)} \quad (3)$$

$$2H_2O + 2e^- \rightarrow H_2 + 2H_2O \text{(Cathodic reaction)} \quad (4)$$

$$Mg + 2H_2O \rightarrow Mg(OH)_2 + H_2 \text{(Overall reaction)} \quad (5)$$

When corrosive solution contain $Cl^{-1}$, $Mg^{2+}$ generated in the anodic reaction will react with $Cl^{-1}$ as following reaction equation

$$Mg^{2+} + 2Cl^{-1} \rightarrow MgCl_2 \quad (6)$$

The corrosion resistance of the $Mg(OH)_2$ film modified AZ91 synthesized with different pH value and time was determined using potentiodynamic polarization tests in 3.5% NaCl solution, as shown in Fig. 9. In a typical polarization curve, lower corrosion current densities correspond to lower corrosion rates and better corrosion resistance [25]. All of the corrosion potential of $Mg(OH)_2$ films increase compared with AZ91 substrate, which means that

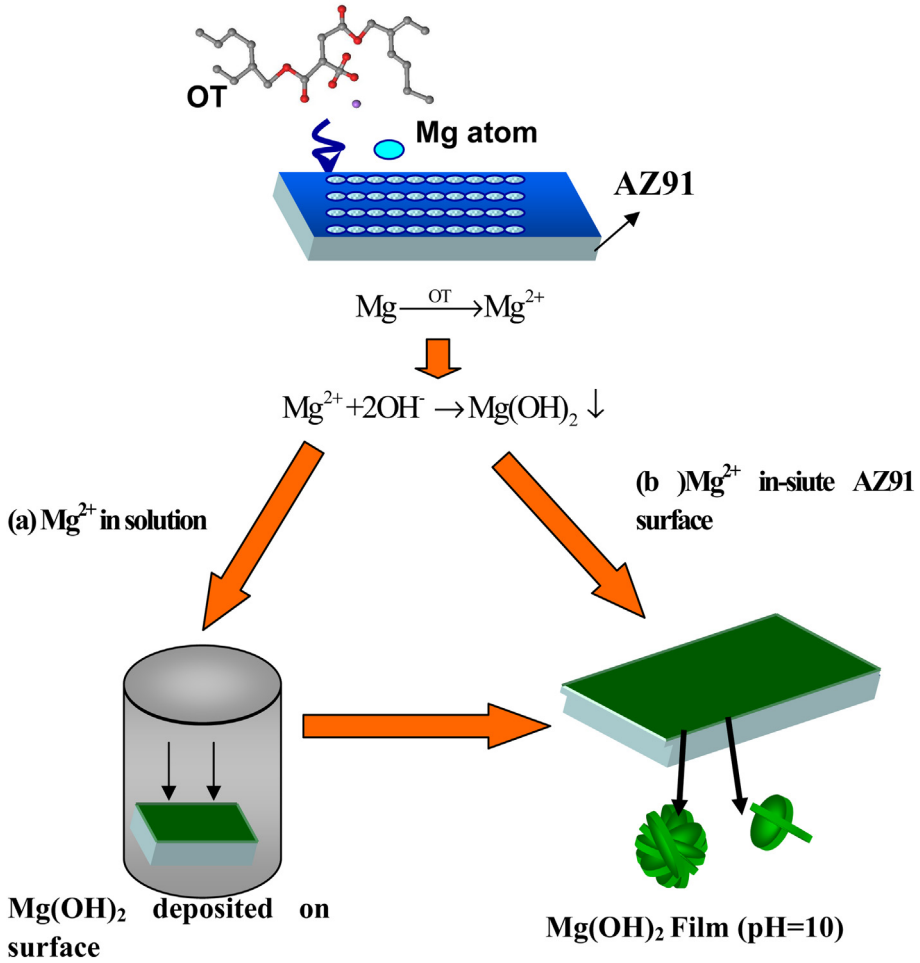


**Fig. 8.** Schematic illustration of the process in the forming $Mg(OH)_2$ film.

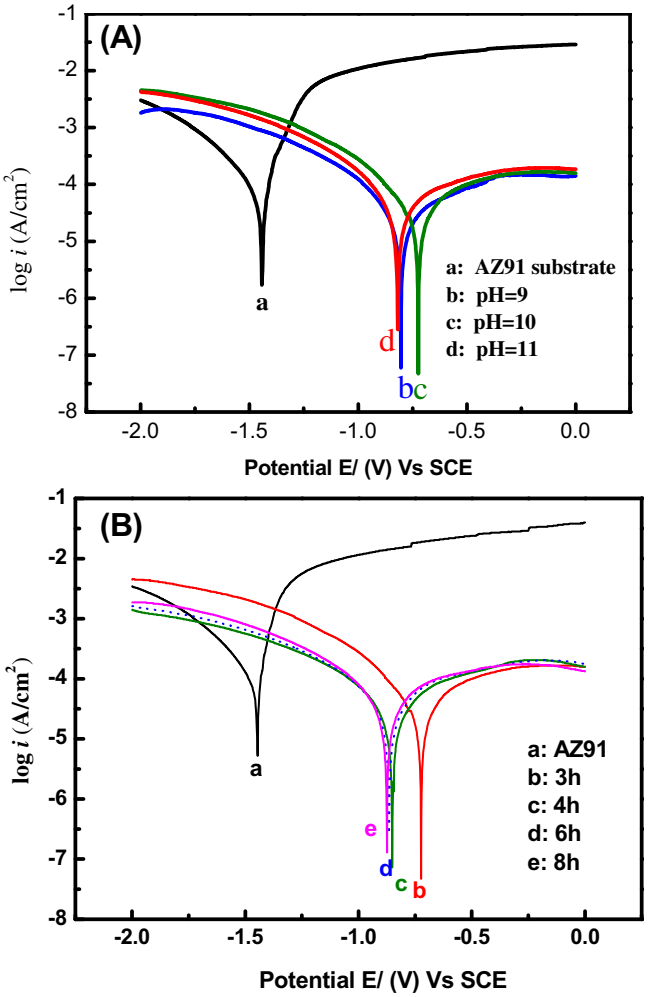


**Fig. 9.** Polarization curves of the bare AZ91 substrate and the $Mg(OH)_2$ films. (A) With different pH values, (B) with different treating time.

the $Mg(OH)_2$ films are very effective in protecting the AZ91 from corrosion. In Fig. 9(A), the $Mg(OH)_2$ film obtained at pH 10 exhibits the highest increase in corrosion potential at −0.7097 V (SCE), while the corrosion potentials of others $Mg(OH)_2$ films are similar. Meanwhile, the $i_{corr}$ of $Mg(OH)_2$ coated AZ91 are approximately one order of magnitude lower than that of the bare AZ91. Fig. 9(B) shows that hydrothermal treatment time is very importance to their corrosion resistance, the film obtained with 3 h shows the highest increase in corrosion potential. Basic on the study, it can be suggest that $Mg(OH)_2$ films can provide adequate protection for the AZ91. The anticorrosion mechanism of obtained $Mg(OH)_2$ film is depicted as Reactions (7) and (8).

$$Mg(OH)_2 \rightarrow Mg^{2+} + 2OH^- \quad K_{sp} = 5.61 \times 10^{-12} \tag{7}$$

$$Mg^{2+} + 2Cl^{-1} \rightarrow MgCl_2 \tag{8}$$

In the solution containing chloride ions, $Mg^{2+}$ dissolved from $Mg(OH)_2$ is so low concentration due to the value of $K_{sp}$ ($Mg(OH)_2$) is small ($5.61 \times 10^{-12}$), that chloride ions can't reaction with $Mg^{2+}$ to generate $MgCl_2$. Taken together, these results show that the $Mg(OH)_2$ film is useful of corrosion protection for Mg alloys.

## 4. Conclusions

The $Mg(OH)_2$ film is successfully grown on the substrate of magnesium alloy AZ91 by an in-situ hydrothermal method. The adherence of the as grown films is strong due to the in-situ growth process. The morphologies of the films are compact and uniform, resulting in better protection for AZ91 substrate. The corrosion resistance of AZ91 substrate coated with $Mg(OH)_2$ films is improved effectively in comparison with the bare AZ91. The results suggest that formation of the $Mg(OH)_2$ films on the Mg alloy substrate can provide a potential material for appropriate orthopedic surgery.

## Acknowledgments

We appreciate the financial support of the Fundamental Research Funds for the Central Universities (HEUCF201310010), Open Research Fund Program of State Key Laboratory of Rare Earth Resource Utilization (RERU2011004) and the National Natural Science Foundation of China (Nos. 51108111, 21203040)

## Appendix A. Supplementary data

Supplementary data related to this article can be found at http://dx.doi.org/10.1016/j.matchemphys.2013.09.005.

## References

[1] Y.J. Zhang, C.C. Yan, F.H. Wang, H.Y. Lou, C.N. Cao, Study on the environmentally friendly anodizing of AZ91D magnesium alloy, Surf. Coat. Technol. 161 (2002) 36–43.
[2] B.L. Mordike, T. Ebert, Magnesium properties-applications-potential, Mater. Sci. Eng. A 302 (2001) 37–45.
[3] J.E. Gray, B. Luan, Protective coatings on magnesium and its alloys-a critical review, J. Alloys Compd. 336 (2002) 88–113.
[4] M.P. Staiger, A.M. Pietak, J. Huadmai, G. Dias, Magnesium and its alloys as orthopedic biomaterials: a review, Biomaterials 27 (2006) 1728–1734.
[5] L.P. Xu, G.N. Yu, E.L. Zhang, F. Pan, K. Yang, In vivo corrosion behavior of Mg–Mn–Zn alloy for bone implant application, J. Biomed. Mater. Res. 83A (2007) 703–711.
[6] M. Niinomi, Recent metallic materials for biomedical applications, Met. Mater. Trans. A 33 (2002) 477–486.
[7] A.U. Simaranov, A. Marshakov, Y.U.N. Mikhailovskii, The composition and protective properties of chromated conversion coatings on magnesium, Prot. Met. 28 (1992) 576–580.
[8] Y.W. Song, D.Y. Shan, E.H. Han, Electrodeposition of hydroxyapatite coating on AZ91D magnesium alloy for biomaterial application, Mater. Lett. 62 (2008) 3276–3279.
[9] F. Hosseinbabaei, B. Raissidehkordi, Electrophoretic deposition of MgO thick films from an acetone suspension, J. Eur. Ceram. Soc. 20 (2000) 2165–2168.
[10] Y. Ge, B. Jiang, Z. Yang, Y. Li, Microstructure and corrosion resistance behavior of composite micro-arc oxidation and $SiO_2$ coatings on magnesium alloys, Adv. Mater. Res. 160–162 (2011) 1834–1838.
[11] L.Y. Niu, Z.H. Jiang, G.Y. Li, C.D. Gu, J.S. Lian, A study and application of zinc phosphate coating on AZ91D magnesium alloy, Surf. Coat. Technol. 200 (2006) 3021–3026.
[12] T. Lei, C. Ouyang, W. Tang, L.F. Li, L.S. Zhou, Enhanced corrosion protection of MgO coatings on magnesium alloy deposited by an anodic electrodeposition process, Corros. Sci. 52 (2010) 3504–3508.
[13] R.F. Zhang, S.F. Zhang, Formation of micro-arc oxidation coatings on AZ91HP magnesium alloys, Corros. Sci. 51 (2009) 2820–2825.
[14] H.F. Guo, M.Z. An, S. Xu, H.B. Huo, Formation of oxygen bubbles and its influence on current efficiency in micro-arc oxidation process of AZ91D magnesium alloy, Thin Solid Films 485 (2005) 53–58.
[15] F. Stippich, E. Vera, G.K. Wolf, G. Berg, C. Friedrich, Enhanced corrosion protection of magnesium oxide coatings on magnesium deposited by ion beam-assisted evaporation, Surf. Coat. Technol. 103–104 (1998) 29–35.
[16] Y.Y. Zhu, G.M. Wu, Y.H. Zhang, Q. Zhao, Growth and characterization of $Mg(OH)_2$ film on magnesium alloy AZ31, Appl. Surf. Sci. 257 (2011) 6129–6137.
[17] J.P. Liu, Y.Y. Li, X.T. Huang, G.Y. Li, Z.K. Li, Layered double hydroxide nano-and microstructures grown directly on metal substrates and their calcined products for application as Li-ion battery electrodes, Adv. Funct. Mater. 18 (2008) 1448–1458.
[18] P. Gao, Y.J. Chen, Y. Wang, Q. Zhang, X.F. Li, M. Hua, A simple recycling and reuse hydrothermal route to ZnO nanorod arrays, nanoribbon bundles,

nanosheets, nanocubes and nanoparticles, Chem. Commun. (2009) 2762–2764.
[19] X.X. Guo, S.L. Xu, L.L. Zhao, W. Lu, F.Z. Zhang, D.G. Evans, X. Duan, One-step hydrothermal crystallization of a layered double hydroxide/alumina bilayer film on aluminum and its corrosion resistance properties, Langmuir 25 (2009) 9894–9897.
[20] D.J. Haders, A. Burukhin, E. Zlotnikov, R.E. Riman, TEP/EDTA doubly regulated hydrothermal crystallization of hydroxyapatite films on metal substrates, Chem. Mater. 20 (2008) 7177–7187.
[21] Y. Bouvier, B. Mutel, J. Grimblot, Use of an Auger parameter for characterizing the Mg chemical state in different materials, Surf. Coat. Technol. 180–181 (2004) 169–173.
[22] L. Qiu, R. Xie, P. Ding, B. Qu, Preparation and characterization of $Mg(OH)_2$ nanoparticles and flame-retardant property of its nanocomposites with EVA, Compos. Struct. 62 (2003) 391–395.
[23] K.S. Choi, H.C. Lichtenegger, G.D. Stucky, Electrochemical synthesis of nanostructured ZnO films utilizing self assembly of surfactant molecules at solid–liquid interfaces, J. Am. Chem. Soc. 124 (2002) 12402.
[24] Y. Tan, M.P. Steinmiller Ellen, K.S. Choi, Electrochemical tailoring of lamellar-structured ZnO films by interfacial surfactant templating, Langmuir 21 (2005) 9618–9624.
[25] J. Wang, D.D. Li, X. Yu, X.Y. Jing, M.L. Zhang, Z.H. Jiang, Hydrotalcite conversion coating on Mg alloy and its corrosion resistance, J. Alloys Compd. 494 (2010) 271–274.